

Power Electronic Converter Control Emulating Synchronous Machine Characteristics for Renewable Energy Integration

Etornam Komla Ahorsu Chinenye Chibueze Vincent Odei Kelvin Mireku Francis Boafo Effah

Department of Electrical and Electronic Engineering
Kwame Nkrumah University of Science and Technology
Kumasi, Ghana

Abstract — The integration of distributed energy resources (DER) generation units based on renewable energy systems into the power system is going on at an unprecedented rate in both bulk power systems and distribution systems globally. However, as the penetration of DER renewables in the power system increases, the system inertia will decline leading to stability issues. As a result, improved converter control methods are required to ensure the high penetration of DERs into the existing power system will not jeopardize the future smart grid. Given that the synchronous generator (SG) has been the bedrock of stable power system operation for over a century, it is desirable for these converter control schemes to emulate the dynamics of the synchronous generator. This idea connotes the virtual synchronous generator (VSG) concept. This paper highlights key findings from recent publications with regard to the VSG concept, by identifying strengths and weaknesses. The inadequacies in some of these literatures are then addressed. A study on the synchronous generator is presented in order to better understand how it controls essential grid parameters. A control technique for an inverter to emulate the SG's droop control and inertia property is then proposed. For performance evaluation, this control technique is simulated in MATLAB/Simulink using closed-loop control of the inverter.

Index Terms — Virtual Synchronous Generator, Renewable Energy, Voltage Source Inverter, Virtual Inertia, Droop characteristics

I. INTRODUCTION

The present power generation system is dominated by huge centralized power plants, such as large thermal and hydroelectric units. These generation plants pose two major challenges. The first has to do with technological and economic issues whereby transmission of electricity from such plants to distant locations, for example, rural areas, would be expensive because substations and long transmission lines with adequate insulation would be employed. The second issue is concerned with the environment. Here, the large thermal power plants that use fossil fuels such as coal, oil, or gas release greenhouse gases such as carbon dioxide (CO₂), which

contribute significantly to climate change. In 2014, the European Union's (EU's) 280 coal plants released 755 million tons of CO₂ – representing around 18 % of the EU's total greenhouse gases [1]. The large-scale adoption of renewable energy (RE) based distributed generation (DG) units has been widely adopted as a promising means of tackling these two challenges. Renewable energy's proportion in the power sector is expected to increase from 25 % in 2017 to 85 % by 2050, primarily due to development in solar and wind power generation [2].

Large synchronous generators (SGs) are mostly used to generate electrical power in traditional centralized power plants. Speed governor and excitation control are utilized in such plants to support power system stability due to inherent rotor inertia. However, most DGs need power electronic interface circuits to connect to the grid but these devices can not inherently provide enough inertia and damping characteristics, due to the lack of a large rotating part. Thus, the inverters lack the flexible voltage regulation and frequency control capability of SGs. Consequently, a high penetration of these inverter-based DGs would make the power system vulnerable to disturbances and system faults. The control of power electronics to emulate the inherent power system control ability of synchronous generators characterizes the virtual synchronous generator (VSG) concept [3]. This paper seeks to design and investigate a power electronic control technique that emulates synchronous machine characteristics to promote power system stability in inverter-dominated grids.

The authors in [4] presented a study of active and reactive power regulation of SGs. To analyze active power regulation of the generator, the input power to the prime mover was adjusted while keeping the field current constant. The power angle (δ) increases as the power due to the electromagnetic torque developed in the generator (P_m) increases. However, [4] did not provide an automatic means of adjusting the power generated by an SG.

A number of papers have provided technical considerations for voltage source inverter (VSI) control scheme design. The authors of [5] presented a specific virtual

synchronous generator (VSG) based on the swing equation of SGs, along with its mathematical model. By measuring grid active and reactive power, the mathematical model provided references for cascaded voltage and current controllers. Virtual impedance was incorporated into their model in order to replicate the quasi-stationary characteristics of synchronous impedance in a conventional SG. MATLAB/Simulink was used to assess the implemented VSG's dynamic reaction to changes in loading. The control scheme adapted in this paper is based on the model implemented in [5]. In [6], a novel control strategy for grid-tied voltage source converters (VSCs) is presented. It comprises a conventional inner current and outer voltage loop, as well as a newly developed inertia function. The virtual inertia loop gives primary frequency support by discharging or charging DC link capacitors of VSCs used in power electronics-based generators such as solar and wind farms. The simulations in [6] revealed that the rate of change of frequency (ROCOF) improved by 23.1% compared to the approach in [7].

The authors in [8] described a control scheme for parallel operation of VSGs allowing them to dispatch transient load proportionally to their individual capacities. The control logic was implemented via a frequency droop-based controller expressed by (1) and achieved by choosing suitable values for parameters K_I and K_p to ensure each of the two VSGs share transient loads according to their respective capacities.

$$P_{VSG} = K_I \frac{d\Delta f}{dt} + K_p \Delta f \quad (1)$$

where P_{VSG} is the power output of the VSG, K_p is the emulated damping constant, K_I is the emulated inertia constant and f is the system frequency.

The damping constant (K_p) equals the slope m_1 which corresponds to the larger VSG is less than that of the smaller VSG (slope m_2). Hence, for the same change in system frequency the larger VSG would pick up more load as compared to the smaller VSG. In [9], four major VSG topologies utilized in renewable energy-based distributed generation (DG) units were compared. These are: VSG-ISE by researchers in Osaka University, VSG-VSYNC by the European VSYNC research group, VSG-VISMA by the Institute of Electrical Power Engineering (IEPE) research group in Germany, and the Synchronverter. The Synchronverter was found to have advantages over the other topologies in that it is capable of greater active power injections into the grid and automatic regulation of active and reactive power via frequency and voltage droop control, respectively. The preferred topology is determined by the desired degree of resemblance to the dynamics of an SG.

The rest of this paper is structured as follows. Section II gives the theoretical design considerations for the adopted VSG control scheme, section III implements the VSG scheme in MATLAB/Simulink, section IV details the methodology used to investigate the effectiveness of the control scheme,

section V presents simulation results and the paper is concluded in section VI.

II. THEORETICAL BACKGROUND

In a synchronous machine (SM) dominated power system, injection of reactive power at a bus causes the voltage to rise whereas absorption of reactive power causes the bus voltage to decline. On the other hand, for a power system dominated by DERs, the voltage at the point of common coupling is influenced by both active and reactive power exchange from the DER [10]. The magnitude of voltage change is dependent on the system short circuit impedance and its X/R ratio.

Power system frequency increases with active power injection and decreases with active power absorption. The magnitude of frequency change depends upon the relative value of active power exchange in comparison with power generation from the remaining generators in the power system.

A steady-state system frequency results when synchronous power generation matches the system load and the losses in power system supplying those loads. In the case of a system disturbance, such as sudden loss of a generation unit, the kinetic energy of all the synchronous machines (including generators, condensers and motors) is autonomously extracted to supply the load, leading to a decline in the speed of generators and consequently the system frequency. The decline in frequency continues until additional power injection from SGs balance out the load. The rate at which the frequency decreases is termed "Rate of Change of Frequency (ROCOF)". The lowest level at which the frequency is eventually arrested is known as the "frequency nadir."

Primary frequency control is provided by synchronous generator turbine governors injecting power from the generators. This causes the frequency to stabilize at a level higher than the nadir but still lower than the steady-state frequency before the disturbance. Secondary frequency control through Automatic Generation Control (AGC) is then exercised to restore system frequency to its pre-disturbance scheduled level [11]. Tertiary frequency control is provided subsequently which involves restoration of the SG and other reserves which provided primary frequency control, to their preset levels, so that they can respond to any future loss-of-generation events. The tertiary control involves coordinated changes in the dispatch levels or outputs of different generators. In this control, some generators are dispatched down to restore their reserves capability while some other generators are dispatched up by a corresponding amount, while maintaining the system frequency [12].

Synchronous inertia is defined as "the ability of a power system to oppose changes in system frequency due to resistance provided by rotating masses" [13]. The system inertia, however, represents the aggregation of kinetic energy stored in the rotating masses of all the SMs (i.e., generators, condensers, and motors) in the system. This system inertia provides the synchronous inertial response to arrest the system frequency as soon as the frequency starts to decline following

the loss of a major generation [14]. The system inertia dictates the initial ROCOF. The ROCOF is proportional to the size of generation loss and inversely proportional to twice the synchronous inertial response.

The rotational inertia is the primary characteristic of synchronous generators lacking in power electronic converters with respect to power generation. In the transient state, whenever the rotor speed of a synchronous generator (ω_m) is different from the synchronous speed (ω_s), a damping torque is produced which according to Lenz's law [15] tries to restore the rotor to synchronous speed. The swing equation captures the inertia and damping properties of the SG, and is given as:

$$J \frac{d\omega_m}{dt} + D_d \Delta\omega_m = \tau_m - \tau_e \quad (2)$$

where J is moment of inertia of rotating masses (turbine and rotor), ω_m is the angular speed of the rotor, ω_s is the synchronous speed, $\Delta\omega = \omega_m - \omega_s$, τ_m is the mechanical torque, τ_e is the electromagnetic torque and D_d is the damping torque coefficient.

Increasing penetration of DERs and the retirement of large conventional thermal synchronous generators is leading to a substantial decline in inertia in power systems which have adverse effects on the future smart grid. Most DER generation units based on renewable energy systems exist within microgrids. Microgrids are a subgroup of low-voltage and medium-voltage distribution systems [16] (4 kV to 35 kV phase to phase). The ratings of DG units in microgrids usually range from 10 kW to 100 MW. Inverters provide two primary functions in microgrid operation: grid-following (GFL) and grid-forming (GFM). The distinction between GFL and GFM is that the former adjusts their output power by detecting and following the angle/frequency of the grid voltage [17]. By contrast, a GFM source actively regulates the frequency and voltage of its output. In GFM inverters, droop control is extensively used to generate frequency and voltage commands based on measured real and reactive power values respectively [17].

An islanded microgrid with GFM inverter operation was chosen for our simulation since it is most suitable for demonstrating the P-f droop and Q-v droop characteristics emulation of synchronous generators in power electronic converters. This affords us the opportunity to set our own reference values for the system voltage and frequency and then control each of these parameters using droop control with the swing equation or virtual inertia (similar to the SG).

The P-f droop characteristic of the VSG is expressed as:

$$F = F_{ref} + K_P(P_{ref} - P) \quad (3)$$

with K_P – droop coefficient, F – frequency of the VSG, F_{ref} – reference grid frequency (50 Hz), P – measured 3-phase active power, and P_{ref} – is the reference active power.

The swing equation is utilized to replicate the inertia and damping property of the SG in power electronic converter

control. The swing equation as applied to the VSG implementation is expressed as:

$$P_{in} - P_{out} = J\Delta F' + D\Delta\omega \quad (4)$$

where J is the inertia coefficient, D is the damping coefficient, P_{in} is the input power from the voltage source, P_{out} is the output power of VSG. Equations (3) and (4) are used in designing the P-f droop control block diagram. The inertia coefficient J reduces the maximum deviation of frequency and gives a smaller ROCOF following a disturbance. Also, D helps to weaken fluctuations and then decreases the settling time of the frequency.

The Q-v droop characteristic of the VSG is expressed as;

$$V_{ref} = V_{nom} + K_v(Q_{nom} - Q_{ref}) \quad (5)$$

where K_v is the droop coefficient, V_{ref} represents the output voltage of the Q-V droop controller, V_{nom} is the nominal grid voltage, Q_{ref} is the measured 3-phase reactive power, and Q_{nom} is the nominal reactive power. Equation (5) is used in designing the Q-v droop control block diagram.

The transfer function expressed by (6) is utilized in emulating the inertia constant J of the conventional synchronous generator.

$$\frac{1}{\tau s + 1} \quad (6)$$

τ is called the delay factor. The higher the value of τ , the longer it takes for the value of the active power measured to change.

III. WORK DONE

A droop controller which comprises active power-frequency (P-f) droop, reactive power-voltage (Q-v) droop and inertia emulation has been designed to regulate grid frequency and inverter output voltage with changes in load. Space Vector PWM (SVPWM) is the modulating technique employed in regulating the voltage source inverter. The block diagram of the control scheme is given in Fig. 1.

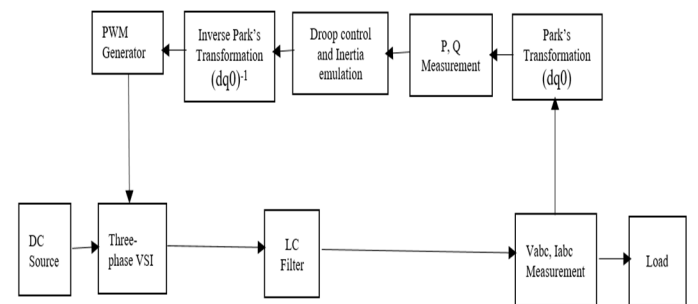


Fig. 1. Block diagram of VSG control scheme

Measurements of voltage and current of the load are taken in the a-b-c reference frame and transformed to dq0 coordinates. The d-q components of the voltage and current values are used to compute the active and reactive powers which are used in (3), (4) and (5) for implementing the droop controllers. The outputs of the controllers were inverse transformed to give the reference voltages for generating the PWM pulses used in controlling the voltage source inverter.

The DC source is coupled to a three-phase inverter, which transforms the DC power to 50 Hz AC power. The LC filter reduces inverter output harmonics and aids in the design of voltage and current controllers. The entire system was implemented in MATLAB/Simulink as shown in Fig. 2.

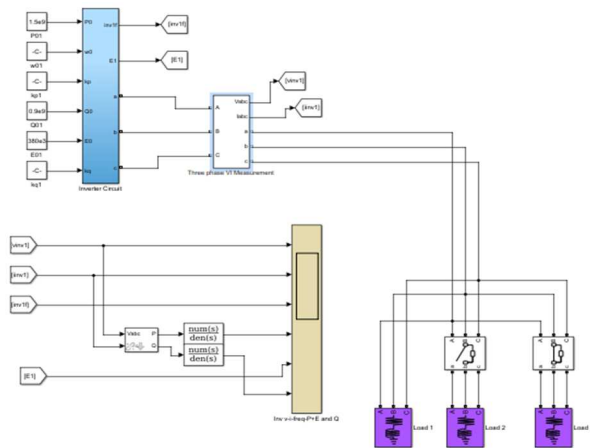


Fig. 1. Simulink design of closed-loop controlled inverter in an island microgrid

IV. TESTING

Two test cases were simulated to assess the proposed closed-loop voltage source inverter (VSI) control scheme in grid-forming islanded microgrid operation. The first case is an open-loop control microgrid model (Case A) while the second case is the proposed closed-loop control microgrid model (Case B).

Table 1 Parameters for modelling case A

Islanded Microgrid Parameters	V_{dc}	L (filter)	C (filter)	Carrier frequency
	1.94 pu	0.27mH	93.8 μ F	2 kHz

Table 2 Parameters for modelling case B

Islanded Microgrid	V_{dc}	L (filter)	C (filter)	Carrier frequency
	1.63 pu	0.02 H	30 μ F	2 kHz
Droop and Voltage Control	K_p	K_q	K_{vp}	K_{vi}
	1.257e-9	6.33e-5	1	50
Current Control and Delay factor	β_p	β_i	τ	
	1	50	0.01	

Droop Control	P_{ref}	Q_{ref}	F_{nom}	V_{nom}
	1 pu	0.6 pu	50 Hz	1 pu

V. RESULTS AND ANALYSIS

Figure 3 depicts the results for case A. When the load is increased, both active and reactive power measured increase; when the load is decreased, both active and reactive power measured fall, this is due to the change in current levels under the different loading conditions. Additionally, the load changes caused the system frequency to drift rapidly. However, because the phase-locked loop (PLL) used to obtain the frequency signal was capable of automatic gain control, the system frequency response may not be accurately represented. The oscillations in frequency and measured active and reactive power in response to load changes indicate the necessity for adding a droop controller to the system in case A.

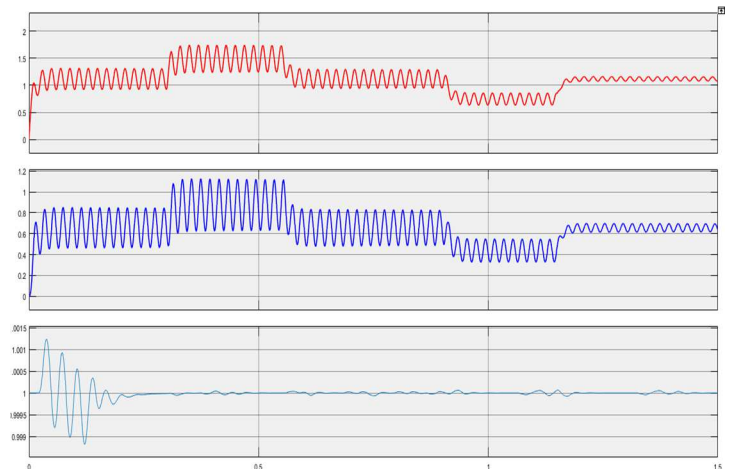


Fig. 3. Active Power (P), Reactive power (Q) and system frequency (f) (from top to bottom) when an impedance (real and reactive) load is switched on from $t = 0.3$ to 0.55 s and switched off from $t = 0.9$ to 1.15 s for case A

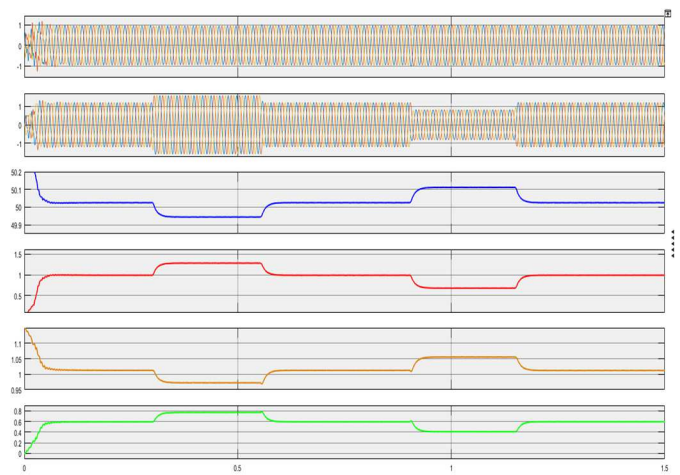


Fig. 4. System voltage (V), current (I), f, P, inverter reference output voltage (E) and Q (from top to bottom) when an impedance (real and

reactive) load is switched on from $t = 0.3$ to 0.55 s and switched off from $t = 0.9$ to 1.15 s for case B

Figure 4 demonstrates the results obtained in case B. The bus voltage or system voltage remains fairly constant throughout the simulation period. When the load increases, the current response reacts immediately increasing from 1.189 pu to 1.463 pu (peak) and decreasing from 1.189 pu to 0.761 pu (peak) when the load was decreased. The inverter reference output voltage also decreases from 0.594 pu to 0.409 pu for the increase in load and increases from 0.594 pu to 0.770 pu for a decrease in the load. The system frequency decreases from 50.02 Hz to 49.92 Hz for the increase in load and increases from 50.02 Hz to 50.11 Hz for a decrease in the load. Figure 4 thus demonstrates the emulation of active power-frequency (P-f) and reactive power – voltage (Q-v) droop characteristics of a SG in a voltage source inverter (VSI) operation. As expected, a change in active power produces an inversely proportional change in frequency. Similarly, a change in reactive power produces an inversely proportional change in inverter reference output voltage.

VI. CONCLUSION

A power electronic converter emulating conventional synchronous machine characteristics has been presented in this paper. Both open-loop and closed-loop control of the voltage source inverter were demonstrated. The open-loop system, which was characterized by power and frequency oscillations, necessitating the need for a controller. The proposed closed-loop control scheme achieved improved power and frequency oscillations and hence better power system stability and operation. The closed-loop control scheme also emulated the conventional synchronous machine in terms of active power control, reactive power control and system inertia. This paper thus demonstrated the active power-frequency (P-f) and reactive power-voltage (Q-v) droop characteristics of a conventional synchronous generator in the operation of a power electronic converter.

Due to the high number of inverter-based DER units anticipated in modern power systems, the proposed VSG idea is expected to be broadly applicable in improving power system stability and controllability.

REFERENCES

- [1] D. Jones and J. et al Huscher, 'Europe' s dark cloud', p. 31, 2016, [Online]. Available: https://www.env-health.org/wp-content/uploads/2018/12/HEAL-Lignite-Briefing-en_web.pdf.
- [2] M. Larsson, Global Energy Transformation. 2009.
- [3] Q.-C. Zhong, Power Electronics-Enabled Autonomous Power Systems. Wiley-IEEE Press, 2020.
- [4] H. Sun, 'Adjustment of Active and Reactive Power of Synchronous Generator in Grid-connected Operation', *IOP Conf. Ser. Earth Environ. Sci.*, vol. 440, no. 3, 2020, doi: 10.1088/1755-1315/440/3/032004.
- [5] S. D'Arco, J. A. Suul, and O. B. Fosfo, 'A Virtual Synchronous Machine implementation for distributed control of power converters in SmartGrids', *Electr. Power Syst. Res.*, vol. 122, pp. 180–197, 2015, doi: 10.1016/j.epsr.2015.01.001.
- [6] M. Saeedian, B. Pournazarian, S. S. Seyedalipour, B. Eskandari, and E. Pouresmaeil, 'Emulating rotational inertia of synchronous machines by a new control technique in grid-interactive converters', *Sustain.*, vol. 12, no. 13, 2020, doi: 10.3390/su12135346.
- [7] Fang, J.; Li, H.; Tang, Y.; Blaabjerg, F. Distributed Power System Virtual Inertia Implemented by Grid-Connected Power Converters. *IEEE Trans. Power Electron.* 2018, 33, 8488–8499. [CrossRef]
- [8] P. Adhikari, S. Prajapati, I. Tamrakar, U. Tamrakar, and R. Tonkoski, 'Parallel operation of virtual synchronous machines with frequency droop control', 2017 7th Int. Conf. Power Syst. ICPS 2017, pp. 116–120, 2018, doi: 10.1109/ICPES.2017.8387278.
- [9] G. Penha da Silva Júnior, T. Figueiredo do Nascimento, and L. Sales Barros, 'Comparison of Virtual Synchronous Generator Strategies for Control of Distributed Energy Sources and Power System Stability Improvement', 2021, doi: 10.48011/sbse.v1i1.2482.
- [10] Pathak, A.K. & Sharma, M.P & Bunde, Mahesh. (2015). A critical review of voltage and reactive power management of wind farms. *Renewable and Sustainable Energy Reviews.* 51. 10.1016/j.rser.2015.06.015.
- [11] Jun Long, Cheng Gong, Yidan Lu. "Tertiary Control of Islanded Microgrids Based on a Linearized ACOF with Losses Compensation", 2019 9th International Conference on Power and Energy Systems (ICPES), 2019
- [12] M. Lomme, 'Modeling of a Microgrid: Power Sharing in Synchronous Generators and Inverters', *Long Range Plann.*, vol. 9, no. 1, p. 92, 2015.
- [13] Inertia: Basic Concepts and Impacts on the ERCOT & PDF fileFigure 4: Correlation between Wind Penetration and Inertia in 2015, 2016 ,and 2017 Generator commitments at any given. (n.d.). Retrieved June 25, 2022, from <https://pdfslide.net/documents/inertia-basic-concept-s-and-impact-s-on-the-ercot-figure-4-correlation-between.html?page=3>
- [14] Denholm, P., Mai, T., Kenyon, R. W., Kroposki, B., & O'malley, M. (2020). *Inertia and the Power Grid: A Guide Without the Spin*. www.nrel.gov/publications.
- [15] M. Choopani, S.H. Hosseinian, B. Vahidi. "A novel comprehensive method to enhance stability of multi-VSG grids", *International Journal of Electrical Power & Energy Systems*, 2019
- [16] Md Hossain, Hemanshu Pota, Walid Issa, Md Hossain. "Overview of AC Microgrid Controls with Inverter-Interfaced Generations", *Energies*, 2017
- [17] D. Pattabiraman, R. H. Lasseter, and T. M. Jahns, 'Comparison of Grid Following and Grid Forming Control for a High Inverter Penetration Power System', *IEEE Power Energy Soc. Gen. Meet.*, vol. 2018-August, pp. 1–5, 2018,